

Experimental Confirmation of Stable, Small-Debye-Length, Pure-Electron-Plasma Equilibria in a Stellarator

J. P. Kremer, T. Sunn Pedersen, R. G. Lefrancois, and Q. Marksteiner

Department of Applied Physics and Applied Mathematics, Columbia University, New York, New York 10027, USA

(Received 5 June 2006; published 1 September 2006)

The creation of the first small-Debye length, low temperature pure electron plasmas in a stellarator is reported. A confinement time of 20 ms has been measured. The long confinement time implies the existence of macroscopically stable equilibria and that the single particle orbits are well confined despite the lack of quasisymmetry in the device, the Columbia non-neutral torus. This confirms the beneficial confinement effects of strong electric fields and the resulting rapid $E \times B$ rotation of the electrons. The particle confinement time is presently limited by the presence of bulk insulating materials in the plasma, rather than any intrinsic plasma transport processes. A nearly flat temperature profile is seen in the inner part of the plasma.

DOI: [10.1103/PhysRevLett.97.095003](https://doi.org/10.1103/PhysRevLett.97.095003)

PACS numbers: 52.27.Jt, 52.27.Aj, 52.55.Hc

Introduction.—Much of the study of non-neutral plasmas has been conducted in Penning-Malmberg traps [1–3] and, to a lesser degree, pure toroidal traps [4–6]. Recently, interest has grown in how such plasmas might behave on magnetic surfaces [7–9]. Theory predicts that the equilibrium, stability, and transport of non-neutral plasmas on magnetic surfaces are fundamentally different from such plasmas in Penning-Malmberg and pure toroidal traps [7,10–12]. The large electric field provided by the space charge of the non-neutral plasma is expected to lead to excellent particle confinement [7,13] on the magnetic surfaces. A non-neutral stellarator may also allow for the study of electron-positron and anti-proton-positron plasmas [14]. The Columbia non-neutral torus (CNT) is the first stellarator designed to study pure electron, partly neutralized, and electron-positron plasmas on magnetic surfaces. In this Letter we describe the first results from pure-electron-plasma experiments on CNT, showing that the stellarator magnetic surfaces have been filled with a well-confined, small-Debye-length, relatively cold, pure-electron plasma. This is the first time that a cold, small-Debye-length, pure-electron plasma has been created in a stellarator. Electron clouds have already been studied in the CHS stellarator [9], but the Debye length was comparable to the minor radius of the plasma, and the temperature was at least an order of magnitude higher than what is reported here.

Experimental description.—CNT is a simple two-period stellarator created by four circular planar coils. Two are interlocking and encased in vacuum jackets within the vacuum chamber and the other two, which act as a Helmholtz coil pair, are outside the vacuum chamber. A computer-aided design drawing of the CNT configuration is shown in Fig. 1. Both the angle between the two interlocking coils (the tilt angle) and the ratio of currents in the interlocking and Helmholtz coils can be varied to explore different magnetic surface topologies. For the studies described in this Letter, the tilt angle is 64° and the ratio of

currents between the interlocking and the Helmholtz coils is 3.64. Field line mapping has confirmed the existence of good magnetic surfaces and an aspect ratio $A \leq 1.9$ [15] for this configuration, lower than any other stellarator. A detailed description of the CNT device can be found in previous publications [16,17].

Injection and diagnostic techniques.—Electrons are injected from a heated, biased tungsten filament placed inside the magnetic surfaces, close to the magnetic axis. A negative bias relative to the vacuum chamber is applied to the emitting filament by a dc power supply. The filament is mounted near the end of a hollow 1.27 cm diameter ceramic rod. The rods and the tables are shown in blue in Fig. 1.

In addition to the measurement of the emission current, which provides the source rate of electrons, the plasma is

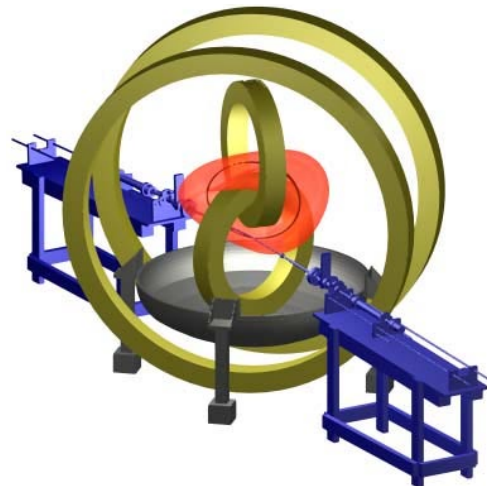


FIG. 1 (color online). A cutaway drawing of the CNT device. The confining volume is shown in red, the coils are shown in yellow, and the filament rods and their tables are shown in blue. The electron emitter rod is positioned such that the emitter is placed on the magnetic axis (black).

diagnosed using filaments similar to the emitter filament. These filaments are used as conventional Langmuir probes when they are cold and emissive probes when they are heated enough to cause thermionic emission—the local plasma potential, electron temperature, and electron density can be determined at each filament. An array of eight filaments spaced 4 cm apart along the length of a ceramic rod identical to the emitter rod is used to measure radial potential, density, and temperature profiles from near the magnetic axis to $\Psi = 0.74$. Here Ψ is a magnetic surface coordinate that increases from 0 on the magnetic axis to 1 on the last closed flux surface. Ψ corresponds to the fractional radial distance from the axis to the last closed flux surface at a separate cross section. The measurement of plasma parameters with probes in a pure-electron plasma is nontrivial due to the large Debye length (generally larger than the probes), the low electron density, and the large space charge of the plasma. The lack of an ion population also makes the floating potential of a nonemissive probe undefined [18]. In addition, for the experiments reported on here, the excellent confinement of the electrons combined with the low electron density poses a challenge in that collection of currents as low as 100 nA may alter the equilibrium or at least deplete local magnetic field lines of electron density. The CNT probe measurement techniques will be briefly summarized here. The details will be presented in a separate article [19].

A fundamental measurement in a non-neutral plasma is the plasma potential profile. As mentioned, the floating potential of a nonemissive (conventional) Langmuir probe is not well defined in a pure-electron plasma due to the lack of an ion current. Instead, two other techniques are used. The first technique is to measure the floating potential of a filament heated sufficiently to produce thermionic emission, i.e., an emissive probe. The floating potential Φ_f of an emissive probe is related to the plasma potential through the electron temperature T_e by $\Phi_f = \Phi_{\text{plasma}} - \alpha T_e/e$, where $\alpha \leq 1$ [20]. The local plasma potential is also measured as the deviation potential—the potential where the hot (emissive) and cold (nonemissive) current-voltage characteristics of a filament begin to deviate [21]. The deviation potential is generally more accurate and works even when the plasma density is negligible [22]. All plasma potentials discussed in this Letter were determined using this method.

The electron temperature profile is determined from the current-voltage characteristics of cold probes in much the same way as is done in neutral plasmas [23]—by varying the probe potential and fitting the measured collection current to the exponential shape $\exp(e\phi/T_e)$ of the electron current from a Maxwellian plasma onto a repelling collector. With a precise knowledge of the plasma potential, the electron density, n_e , can also be derived from this characteristic—the current to the probe when the probe is at the plasma potential is $I_{\text{probe}} \approx en_e \bar{v} A$, where \bar{v} is the average Maxwellian electron velocity, $\bar{v} = 2\sqrt{2T_e/\pi m_e}$,

and A is the probe collection area. In practice, there is a relatively large uncertainty in the electron density. This is partly because the collected currents are very small and partly because the small uncertainty in plasma potential gives rise to a significantly larger uncertainty in electron density, due to the exponential dependence.

Results.—The first experiments described here were performed at a magnetic field of $B = 0.02$ T, and an emitter bias of $V_{\text{emitter}} = -200$ V. The neutral pressure was $p_n = 2 \times 10^{-8}$ Torr. The radial electron temperature profile is shown in Fig. 2. The profile is essentially flat at about 4 eV in the inner part of the plasma, $\Psi < 0.7$. At $\Psi = 0.74$, it increases to approximately 9 eV. Other measurements from the region $\Psi > 0.8$ indicate that the temperature further increases with minor radius to over 30 eV near the last closed flux surface, $\Psi = 1$.

Electron density in CNT has been measured directly through local probe measurements and indirectly through the measurement of the potential profile. For the experimental parameters described above, a directly measured 1D density profile is shown in Fig. 3. A spline routine was used to produce smoothed 1D temperature and density profiles consistent with the measured values. These are shown as red lines in Figs. 2 and 3, respectively. From these, a full 3D equilibrium reconstruction was performed using the CNT 3D equilibrium Poisson-Boltzmann Solver (PBS) code [10]. The reconstructed potential profile along the length of the probe array is shown with the measured deviation potential profile in Fig. 4. There is excellent agreement between the measured and reconstructed potential profile. The resulting volume averaged density in the reconstructed equilibrium is $n_e = 7.5 \times 10^{11} \text{ m}^{-3}$ thus the total number of electrons confined $N \approx 1.0 \times 10^{11}$.

These measurements imply that the Debye length for these plasmas is $\lambda_D \approx 1.7$ cm. The average minor radius of CNT is $a \approx 15$ cm thus $\lambda_D/a \ll 1$; the plasma criterion has been satisfied. In addition, the results show that a low-temperature, small-Debye-length plasma can be created in a stellarator from a single small emitter. In Penning traps

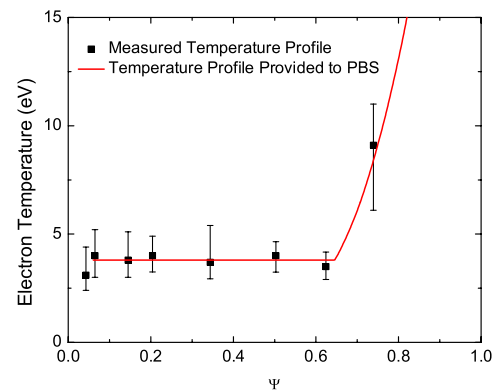


FIG. 2 (color online). The radial electron temperature profile. The temperature is flat at approximately 4 eV for most of the confining region but increases past $\Psi \approx 0.7$. The temperature profile used in the potential reconstruction is shown in red.

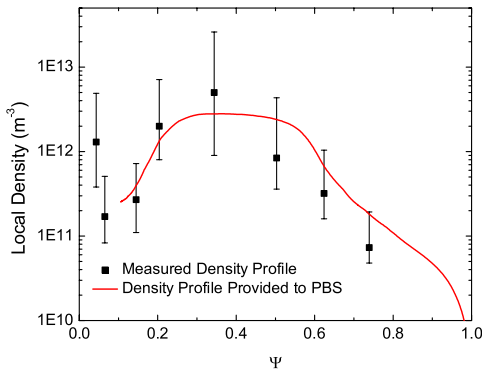


FIG. 3 (color online). Local electron density measurements at each probe. The density profile used in the potential reconstruction is shown in red.

and pure toroidal field traps, filaments must fill the entire cross sectional area and be wound carefully in a spiraling pattern so the filament voltage drop matches a possible potential profile of the pure-electron plasma. This is necessary both to fill the field lines and to achieve low temperature and a large number of Debye lengths [2]. The low temperatures achieved in CNT are important not only because they create a short Debye length, but because they reduce the rate of ionization of neutrals, and hence, the degree of ion contamination. This is a critical issue for an electron plasma confined in a stellarator, which, unlike an electron Penning trap, also confines ions. The ion confinement can be used to study plasmas at any degree of neutralization, but must obviously be avoided when studying pure electron plasmas. The ion fraction has been determined by measurement of the ion saturation current to a large probe constructed for this purpose. For the experiments described here, the ion fraction is $<1\%$, so the plasmas being studied are essentially pure electron plasmas.

The steady-state emission current from the electron emitter for these experiments was $I_e = 1.5 \mu\text{A}$, and therefore, the electron confinement time was $\tau_c \approx eN/I_e \approx 10 \text{ ms}$. Experiments at $B = 0.1 \text{ T}$ but with a neutral pres-

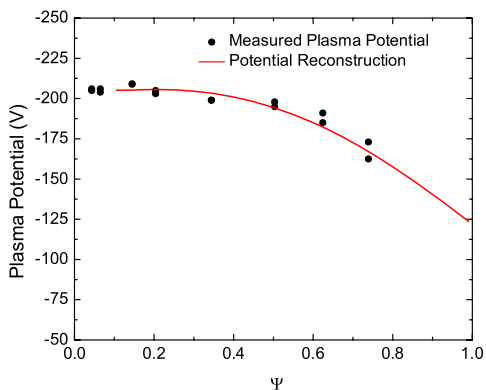


FIG. 4 (color online). Local plasma potential measurements (deviation potential) are shown as black dots. The potential profile of the equilibrium reconstruction is shown as a solid red line.

sure of $p_n = 5 \times 10^{-9} \text{ Torr}$ result in a similar electron inventory but an emission current of $I_e = 0.75 \mu\text{A}$ yielding a confinement time of $\tau_c \approx 20 \text{ ms}$. This is the longest confinement time yet measured. An increase in emitter bias or neutral pressure or, as discussed later, the addition of more insulating rods or a decrease in magnetic field all result in diminished confinement. Comparisons of these confinement times with estimates of relevant time scales prove a pure-electron-plasma equilibrium has been established and that it is macroscopically stable. The time scale for equilibrium on a magnetic surface to be established can be estimated as the time it takes thermal particles to traverse the surface toroidally and poloidally $\tau_{\text{eq}} \approx 2\pi R/(\iota v_{\text{th}})$, where R is the major radius, ι is the rotational transform, and v_{th} is the electron thermal velocity. For the present configuration of CNT with $T_e \approx 4 \text{ eV}$, this is $\tau_{\text{eq}} \approx 10 \mu\text{s}$. Because the confinement time is 3 orders of magnitude larger than the equilibrium time scale, equilibrium has been established on each magnetic surface. This confinement time is orders of magnitude longer than the $E \times B$ rotation period of approximately $50 \mu\text{s}$ using $B = 0.1 \text{ T}$ and a radial electric field estimated from measured radial potential drop across the plasma with an emitter bias of -200 V . This is also the characteristic time scale for particle losses due to large scale electrostatic instabilities, which can therefore be ruled out. The theoretical prediction of the existence of macroscopically stable equilibria of electron plasmas on magnetic surfaces has therefore been confirmed. Moreover, for $B = 0.1 \text{ T}$ the time for a particle to drift out of the confining region due to ∇B drifts is $\tau_{\nabla B} \approx v_{\nabla B}/a \approx 1 \text{ ms}$, so the measured confinement time shows that the vast majority of particles are on confined orbits. This was expected because the strong $E \times B$ drift forces particles to rotate poloidally and therefore prevents them from drifting out, unlike what is observed in classical stellarators confining neutral plasma, where there are significant prompt orbit losses. For $T_e = 4 \text{ eV}$, $n_e \approx 10^{12} \text{ m}^{-3}$ and $p_n = 5 \times 10^{-9} \text{ Torr}$ of nitrogen, electron-electron and electron-neutral collision times are estimated to be $\nu_{ee} \approx 0.2 \text{ s}$ and $\nu_{en} \approx 0.05 \text{ s}$. At $p_n = 2 \times 10^{-8} \text{ Torr}$, $\nu_{en} \approx 0.01 \text{ s}$. The Maxwellian or exponential shape of the collection current therefore implies that the electron plasma has moved into a thermal equilibrium much faster than what can be understood from collisional processes.

Although the confinement time is very long compared to the time scales relevant for parallel force balance and macroscopic stability, it is much shorter than the confinement time predicted from neoclassical transport in the presence of a strong electric field— $\tau_c \approx (a/\lambda_D)^4 \tau_e \approx 10^3 \text{ s}$ [7], where τ_e is the electron collision time. The primary source of transport is the presence of the insulating rods used to hold the emitter and probe filaments. This was determined in a series of experiments where the emission current was measured as a function of magnetic field strength with either one or two rods inserted into the plasma. The experiments were done at a fixed emitter

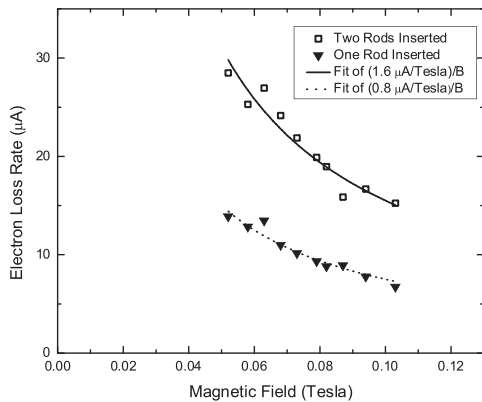


FIG. 5. The emission current (electron loss rate) is seen to increase by a factor of 2 when a second ceramic rod is inserted. Whether one or two rods are present, the emission current scales as $1/B$, implying that the confinement time scales as B .

bias of -400 V so that the electron inventory was held roughly constant. The emission current is therefore inversely proportional to the confinement time. Results are shown in Fig. 5. The emission current when two rods are present is approximately twice the emission current when one rod is present, so two rods cause twice as much radial transport as one rod. Whether one or two rods is present, the emission current scales as $1/B$, consistent with $E \times B$ and/or Bohm scaling. It is believed that the transport results from the electrostatic perturbation caused by the rods. Because of the thermal motion of the electrons, the insulating rods charge up negatively relative to the plasma. The electric field from this charging sets up an $E \times B$ flow pattern that effectively creates a convection cell from the core of the plasma to the edge, and it therefore allows electrons to drift out radially. The measured $1/B$ scaling is consistent with this transport mechanism.

Although the rods are the dominant sources of transport for the experiments reported above, neutrals are observed to create cross-surface transport at higher neutral pressures. Emission current has an offset linear dependence on neutral pressure with the slope and offset determined by the magnetic field strength and emitter bias. These observations are consistent with a neutral driven transport mechanism acting in addition to the rod driven transport. A pneumatic retractable emitter is now under construction which will allow for the creation of electron plasmas without material objects remaining in the confining region. Measurements of electron inventory and potential fluctuations of these plasmas will be provided by a sectored conductor which conforms to the edge of the entire confining region.

Summary.—The densities and temperatures attained in CNT show that many Debye lengths of pure-electron plasma have been confined, that is, the plasma criterion has been well satisfied. A comparison of the measured particle confinement time of 20 ms with relevant single particle confinement time scale confirms the theoretical prediction that macroscopically stable equilibria of electron plasmas on magnetic surfaces exist. Despite having

only a single, pointlike electron source, the electrons fill the plasma volume and the electron plasma temperature is low across most of the plasma profile. The ion fraction is negligible for these experiments due to a combination of good vacuum and a low electron temperature. Electron transport is seen to be dominated by the electrostatic perturbation caused by bulk insulating materials in the confining region.

The authors acknowledge Jack Berkery for useful discussions. This work was supported by the United States DOE Grant No. DE-FG02-02ER54690, the NSF-DOE Partnership in Basic Plasma Science, Grant No. NSF-PHY-03-17359, and the NSF CAREER program, Grant No. NSF-PHY-04-49813.

- [1] R. C. Davidson, *Physics of Nonneutral Plasmas* (Imperial College Press and World Scientific Publishing, London, UK, 2001), 2nd ed.
- [2] J. H. Malmberg and J. S. deGrassie, *Phys. Rev. Lett.* **35**, 577 (1975).
- [3] C. F. Driscoll, J. H. Malmberg, and K. S. Fine, *Phys. Rev. Lett.* **60**, 1290 (1988).
- [4] M. R. Stoneking, M. A. Growdon, M. L. Milne, and R. T. Peterson, *Phys. Rev. Lett.* **92**, 095003 (2004).
- [5] J. D. Daugherty, J. E. Eninger, and G. S. Janes, *Phys. Fluids* **12**, 2677 (1969).
- [6] P. Zaveri, P. I. John, K. Avinash, and P. K. Kaw, *Phys. Rev. Lett.* **68**, 3295 (1992).
- [7] T. S. Pedersen and A. H. Boozer, *Phys. Rev. Lett.* **88**, 205002 (2002).
- [8] H. Saitoh *et al.*, *Phys. Rev. Lett.* **92**, 255005 (2004).
- [9] H. Himura *et al.*, *Phys. Plasmas* **11**, 492 (2004).
- [10] R. G. Lefrancois, T. S. Pedersen, A. H. Boozer, and J. P. Kremer, *Phys. Plasmas* **12**, 072105 (2005).
- [11] A. H. Boozer, *Phys. Plasmas* **12**, 034502 (2005).
- [12] A. H. Boozer, *Phys. Plasmas* **12**, 104502 (2005).
- [13] T. Sunn Pedersen, in *New Developments in Nuclear Fusion Research*, edited by Y. Nakamura (Nova Science Publishers, Hauppauge, NY, 2006).
- [14] T. S. Pedersen *et al.*, *J. Phys. B* **36**, 1029 (2003).
- [15] T. S. Pedersen *et al.*, *Phys. Plasmas* **13**, 012502 (2006).
- [16] T. S. Pedersen *et al.*, *Fusion Sci. Technol.* **46**, 200 (2004).
- [17] T. S. Pedersen *et al.*, *Fusion Sci. Technol.* (to be published).
- [18] H. Himura, C. Nakashima, H. Saitoh, and Z. Yoshida, *Phys. Plasmas* **8**, 4651 (2001).
- [19] J. P. Kremer, T. S. Pedersen, Q. Marksteiner, R. G. Lefrancois, and M. Hahn, *Rev. Sci. Instrum.* (to be published).
- [20] M. Y. Ye and S. Takamura, *Phys. Plasmas* **7**, 3457 (2000).
- [21] F. F. Chen, in *Plasma Diagnostics Techniques*, edited by R. H. Huddlestone and S. I. Leonard (Academic, New York, 1965), p. 113.
- [22] M. H. Cho, C. Chan, N. Hershkovitz, and T. I. Intrator, *Rev. Sci. Instrum.* **55**, 631 (1984).
- [23] I. H. Hutchinson, *Principles of Plasma Diagnostics* (Cambridge University Press, Cambridge, England, 2002), 2nd ed.